Fibre-based fluorescence-lifetime imaging microscopy: a real-time biopsy guidance tool for suspected lung cancer

Susan Fernandes[1,2]^, Elvira Williams[1], Neil Finlayson[1,3]^, Hazel Stewart[1]^, Catharine Dhaliwal[4], David A. Dorward[1,5], William A. Wallace[5], Ahsan R. Akram[1,2]^, James Stone[1,6]^, Kevin Dhaliwal[1,2]^, Gareth O. S. Williams[1]^

[1]Translational Healthcare Technologies Group, Centre for Inflammation Research, Institute for Regeneration and Repair, The University of Edinburgh, Edinburgh, UK; [2]Department of Respiratory Medicine, NHS Lothian, Royal Infirmary of Edinburgh, Edinburgh, UK; [3]Institute for Integrated Micro and Nano Systems, School of Engineering, The University of Edinburgh, Edinburgh, UK; [4]Department of Pathology, NHS Lothian, Western General Hospital, Edinburgh, UK; [5]Department of Pathology, NHS Lothian, Royal Infirmary of Edinburgh, Edinburgh, UK; [6]Centre for Photonics and Photonic Materials, Department of Physics, The University of Bath, Bath, UK

Correspondence to: Gareth O. S. Williams, PhD. Translational Healthcare Technologies Group, Centre for Inflammation Research, Institute for Regeneration and Repair, The University of Edinburgh, 4-5 Little France Drive, Edinburgh, EH16 4UU, UK. Email: G.O.S.Williams@ed.ac.uk; Kevin Dhaliwal, MD, PhD. Translational Healthcare Technologies Group, Centre for Inflammation Research, Institute for Regeneration and Repair, The University of Edinburgh, 4-5 Little France Drive, Edinburgh, EH16 4UU, UK; Department of Respiratory Medicine, NHS Lothian, Royal Infirmary of Edinburgh, 51 Little France Crescent, Edinburgh, EH16 4SA, UK. Email: kev.dhaliwal@ed.ac.uk.

Abstract: Lung cancer is the most common cause of cancer-related deaths worldwide. Early detection improves outcomes, however, existing sampling techniques are associated with suboptimal diagnostic yield and procedure-related complications. Autofluorescence-based fluorescence-lifetime imaging microscopy (FLIM), a technique which measures endogenous fluorophore decay rates, may aid identification of optimal biopsy sites in suspected lung cancer. Our fibre-based fluorescence-lifetime imaging system, utilising 488 nm excitation, which is deliverable via existing diagnostic platforms, enables real-time visualisation and lifetime analysis of distal alveolar lung structure. We evaluated the diagnostic accuracy of the fibre-based fluorescence-lifetime imaging system to detect changes in fluorescence lifetime in freshly resected *ex vivo* lung cancer and adjacent healthy tissue as a first step towards future translation. The study compares paired non-small cell lung cancer (NSCLC) and non-cancerous tissues with gold standard diagnostic pathology to assess the performance of the technique. Paired NSCLC and non-cancerous lung tissues were obtained from thoracic resection patients (N=21). A clinically compatible 488 nm fluorescence-lifetime endomicroscopy platform was used to acquire simultaneous fluorescence intensity and lifetime images. Fluorescence lifetimes were calculated using a computationally-lightweight, rapid lifetime determination method. Fluorescence lifetime was significantly reduced in *ex vivo* lung cancer, compared with non-cancerous lung tissue [mean ± standard deviation (SD), 1.79±0.40 *vs.* 2.15±0.26 ns, P<0.0001], and fluorescence intensity images demonstrated distortion of alveolar elastin autofluorescence structure. Fibre-based fluorescence-lifetime imaging demonstrated good performance characteristics for distinguishing lung cancer, from adjacent non-cancerous tissue, with 81.0% sensitivity and 71.4% specificity. Our novel fibre-based fluorescence-lifetime imaging system, which enables label-free imaging and quantitative lifetime analysis, discriminates *ex vivo* lung cancer from adjacent healthy tissue. This minimally invasive technique has potential to be translated as a real-time biopsy guidance tool, capable of optimising diagnostic accuracy in lung cancer.

Keywords: Lung cancer; diagnostic imaging; optical imaging; interventional pulmonology; fibre-optics

^ ORCID: Susan Fernandes, 0000-0001-5966-4010; Neil Finlayson, 0000-0003-1598-9563; Hazel Stewart, 0000-0002-1619-7202; Ahsan R. Akram, 0000-0003-4605-1682; James Stone, 0000-0002-3420-9860; Kevin Dhaliwal, 0000-0002-3925-3174; Gareth O. S. Williams, 0000-0002-8392-7471.

Introduction

Lung cancer is the most common cause of cancer-related deaths worldwide (1). Low-dose computed tomography screening reduces lung cancer mortality by 20–24% through early detection and treatment (2,3), therefore, it is likely that national screening initiatives will be implemented in the future. Confirmatory histological diagnosis is recommended prior to commencing radical treatment (4). Recent advances in bronchoscopic techniques, such as navigation bronchoscopy (5) and robotic-assisted bronchoscopy (6,7), mean it is now possible to access the majority of peripherally-located pulmonary lesions. The combined application of multiple bronchoscopic techniques, including navigation bronchoscopy and radial endobronchial ultrasound (EBUS), delivers a higher diagnostic yield than each method alone (8). Multimodal bronchoscopy, which integrates real-time image guidance tools, optimises diagnostic accuracy in peripheral pulmonary lesions (8,9) by confirming proximity to target lesion prior to biopsy tool deployment.

Fibre-based optical techniques, which are deliverable via existing endoscopic platforms and add ~10 minutes to conventional procedures (10), have the capability to augment targeted conventional biopsies in lung cancer and mesothelioma (11,12). Fibre-based optical endomicroscopy (OEM) enables high-resolution imaging of distal lung alveolar structure through the autofluorescence of elastin (10,13), which represents 50% of peripheral lung connective tissue fibres (14). Label-free fibre-based OEM, in conjunction with navigation bronchoscopy, has been used to access and identify solitary pulmonary nodules *in vivo* (13,15). However, benign and malignant nodules are often indistinguishable, as both demonstrate abnormal elastin fibre architecture.

Fluorescence-lifetime imaging microscopy (FLIM) is an emerging modality for detecting malignancy (16). This functional imaging technique senses changes in the cellular microenvironment by measuring endogenous fluorophore decay rates. FLIM can generate highly-resolved images by assigning each pixel a colour according to its lifetime value, thereby enabling accurate localisation of abnormal tissue (17). Traditionally, fluorescence lifetime techniques have been relatively slow, however, this has been overcome by recent advances in sensor technology enabling high-throughput FLIM imaging (18,19), thereby making this technology very attractive for translation into the clinical setting. Fibre-based FLIM has shown great promise in discriminating cancer from adjacent healthy tissue (20,21). Indeed, fibre-based FLIM has been integrated into robotic surgery platforms to augment the surgical field of view (22) and deliver real-time feedback, enabling rapid intra-procedure margin assessment in head and neck surgery (23). The application of bench-top FLIM demonstrates excellent sensitivity and specificity for detection of human lung cancer using frozen or paraffin-embedded tissue sections, however, tissue processing techniques affect both fluorescence intensity and lifetime (24,25).

We propose that a fibre-based FLIM system, which enables rapid fluorescence lifetime calculation and visualisation when using a computationally lightweight approach (26) can discriminate between *ex vivo* cancerous and non-cancerous lung tissue as the basis for clinical translation. This minimally invasive, label-free technique is deliverable via existing endoscopic platforms, thereby permitting access to the distal lung parenchyma. As a step towards future translation, we demonstrate proof-of-concept of fibre-based FLIM in freshly resected *ex vivo* human lung cancer. We show that rapid FLIM analysis enables differentiation between cancerous and adjacent non-cancerous lung tissue. We present this article in accordance with the STARD reporting checklist (available at https://tlcr.amegroups.com/article/view/10.21037/tlcr-23-638/rc).

Methods

Ex vivo lung tissue

Patients were identified through regional thoracic surgery centre (Royal Infirmary of Edinburgh) if they were scheduled for resection between October 2018 and August 2019. Patients were deemed eligible if they had suspected or confirmed cancer due for surgical resection with primary tumours ≥3 cm and formed a convenience series. The ground truth of the samples for the purpose of referencing was performed by a diagnostic pathology laboratory. This is
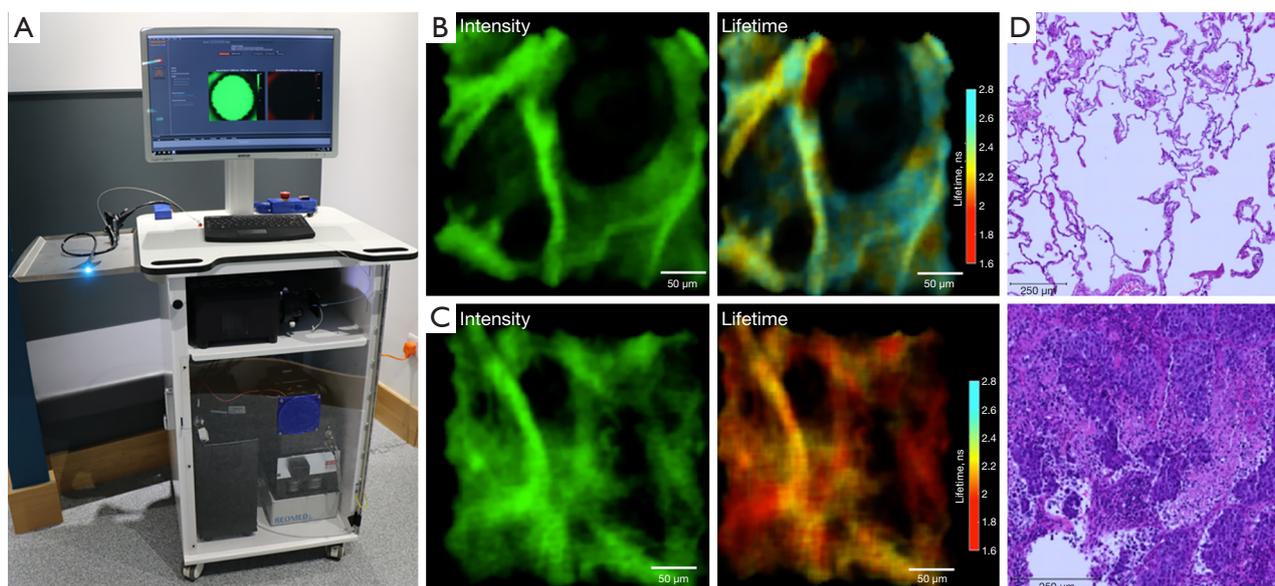
Figure 1 Fluorescence lifetime imaging system and representative images. (A) Fluorescence lifetime imaging platform. (B) Representative fluorescence lifetime imaging of healthy tissue. (C) Representative imaging of cancerous tissue. (D) Corresponding histology images (haematoxylin and eosin stained).

the gold standard method.

Paired fresh cancerous and adjacent non-cancerous lung tissues (>5 cm from tumour margin) were obtained from patients undergoing thoracic resection for lung cancer. The study was approved by NHS Lothian Bioresource Research Ethics Committee (NHS Lothian, reference 15/ES/0094). All study participants gave written informed consent, and the study was conducted in accordance with the provisions of the Declaration of Helsinki (as revised in 2013).

Fibre-based FLIM system

Imaging was performed prospectively using a FLIM microendoscopy platform, which incorporates a confocal laser scanning system and 512 spectral channel time correlated single photon counting sensor capable of "on-chip" histogramming in each channel (27) (*Figure 1A*). This clinically compatible system, which is based upon a benchtop, full-spectral FLIM platform [as described previously (28)], uses a supercontinuum laser (SuperK EVO, NKT Photonics, Denmark) filtered to 488 nm excitation wavelength and has a spectral detection range of 500–760 nm. To increase imaging frame rate, reduce data burden and increase signal to noise, the sensor was binned to two spectral channels (500–580 and 610–760 nm) before transmission to the computer. An approved-for-

clinical-investigation coherent fibre imaging bundle (29) was placed in direct contact with each tissue sample and at least three regions of interest were evaluated. Fluorescence intensity and lifetime video sequences (50 frames) were simultaneously recorded using 128×128 pixel images (350 µm × 350 µm field of view) matching the optical fibre bundle characteristics with an average fibre core oversampling of 4×. The spectral emission range of 500–580 nm was selected for optimal fluorescence lifetime analysis of lung tissue autofluorescence. Lifetime decays were calculated using a rapid lifetime determination method (26), which assumes a single exponential decay, and enables real-time imaging at three frames per second.

A 200-count threshold was applied, which equated to a signal to noise ratio of 4:1, below which the lifetime data was discarded. Fluorescence lifetime images were processed with a transparency weighted by the fluorescence intensity to modulate pixel saturation and optimise visibility of structurally related detail (28). For each fluorescence lifetime video sequence, a distribution histogram of all pixels in the final frame was generated and mean fluorescence lifetime value was calculated using offline MATLAB R2019a (RRID:SCR_001622; MathWorks Inc., Natick, USA). For differentiation of tissue type, a global fluorescence lifetime cut-off value was determined based on the receiver operating characteristic (ROC).

Table 1 Demographics of patients with non-small cell lung cancer (N=21)

Characteristics	Value
Age (years)	68 [53–79]
Sex	
Male	11 [52]
Female	10 [48]
Smoking	
Never	2 [10]
Ex-smoker	16 [76]
Current smoker	3 [14]
Histology	
Adenocarcinoma	11 [52]
Solid pattern	5 [45]
Acinar	3 [27]
Lepidic	3 [27]
Squamous cell carcinoma	6 [29]
Mixed	3 [14]
Pleomorphic carcinoma	1 [5]
Pathologic stage	
I	3 [14]
II	11 [52]
III	5 [24]
IV	2 [10]

Data are presented as N [%] or median [range].

Statistical analyses

Data are presented as mean ± SD. A paired Student's *t*-test was performed to compare patient-matched non-cancer and lung cancer tissue samples. For comparisons among three or more groups, one-way analysis of variance (ANOVA) was performed. Homogeneity of variation among the groups was evaluated using Brown-Forsythe test, prior to applying ANOVA. Exact P values were computed, all P values were two-tailed and P value of <0.05 was considered statistically significant. GraphPad Prism Version 8 (GraphPad Software, Boston, USA) was used for statistical analyses.

Results

Fibre-based FLIM was performed on 21 fresh *ex vivo* lung resection specimens, from patients with stage IB–IVA NSCLC. Patient characteristics are presented in *Table 1*. Fluorescence intensity images of adjacent non-cancerous lung tissue demonstrated normal human alveolar structure, characterised by network of elastin fibres encircling alveolar ducts (*Figure 1B*). Whereas fluorescence intensity images of lung cancer, confirmed with histopathology, demonstrated disorganisation of the elastin fibre architecture with increased elastin fibre thickness and density (*Figure 1C,1D*).

Real-time fluorescence lifetime images were acquired simultaneously, with corresponding histograms of fluorescence lifetime distribution across the whole image. Fluorescence lifetime was significantly reduced in lung cancer, compared with non-cancerous lung tissue (mean ± SD, 1.79±0.40 *vs.* 2.15±0.26 ns, P<0.0001), using fibre-based FLIM. Furthermore, mean fluorescence lifetimes of paired non-cancerous and cancerous lung tissue samples demonstrated a universal downward trend (*Figure 2A*). There was no significant difference in lung cancer fluorescence lifetimes with respect to lung cancer histological subtype, analysed using a one-way ANOVA (P=0.80). ROC analysis demonstrated the optimal global fluorescence lifetime cut-off value for differentiating cancer from adjacent non-cancerous lung tissue, using fibre-based FLIM, was 2.14 ns (sensitivity 81.0% and specificity 71.4%), with area under the curve 0.79 (95% confidence interval: 0.65–0.93) (*Figure 2B*).

Discussion

We report the application of a high-resolution fibre-based FLIM system to discriminate freshly resected *ex vivo* lung cancer, from adjacent non-cancerous tissue, with high sensitivity and good specificity. This novel microendoscopy platform enables both tissue visualisation, through endogenous elastin autofluorescence, and lifetime analysis of lung cancer, which was characterised by abnormal alveolar structure and significantly shorter fluorescence lifetime, compared with non-cancerous lung tissue. The outcomes of this study demonstrate the advanced tissue imaging capabilities of fibre-based FLIM, which has the potential to augment conventional biopsies in patients with suspected lung cancer, by confirming lesion localisation prior to biopsy tool deployment and increasing the biopsy "hit-rate". We envisage the application of this technology particularly for peripheral lung nodules or masses to provide real time feedback that the lesion has been reached and where tools such as EBUS are typically not used. Furthermore, there is
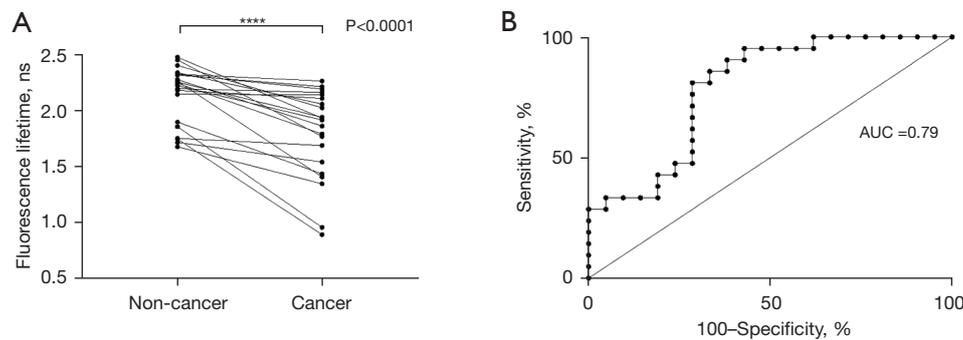
Figure 2 Discrimination of non-cancerous and cancerous tissue by fluorescence lifetime. (A) Fluorescence lifetime trend between non-cancerous and cancerous tissue (****, P<0.0001). (B) Receiver operator characteristic curve for discrimination of lung cancer from non-cancerous tissue. AUC, area under the curve.

potential for the use of the tool to assess the margins of a lesion following resection when coupled with an appropriate bronchoscopy navigation tool.

To date, exogenous fluorescent contrast agents, such as fluorescein and methylene blue, have been used to enhance cellular structure imaging in fibre-based OEM to aid the detection of lung malignancy (11,30). However, there are inherent challenges in the clinical implementation of exogenous fluorophores, such as the requirement for bespoke excitation wavelengths (30), suboptimal target site delivery of topical agents, and adverse reactions associated with systemic administration (31).

We have harnessed the potential of 488 nm excitation to enable label-free dual modality optical fingerprinting of human lung cancer. This fibre-based FLIM system integrates high-resolution autofluorescence confocal imaging with rapid fluorescence lifetime analysis, which enables real-time visualisation of disorganised fluorescent alveolar structure and altered lifetime associated with lung cancer. Furthermore, this flexible, minimally invasive technique is deliverable via existing endoscopic platforms to enable access to small peripherally-located lung lesions.

This proof-of-concept study characterises fluorescence lifetime properties of *ex vivo* human lung tissue, however, optical signatures may be influenced by physiological features of the *in vivo* environment, such as perfusion and ventilation. FLIM has been demonstrated as an *in-vivo* tool for distinguishing cancer from non-cancerous tissue by Hassan *et al.* for the oropharynx (21) with Marsden *et al.* demonstrating fluorescence lifetime trends of healthy and cancerous oral tissue *in vivo* are unchanged, compared with freshly resected *ex vivo* tissue samples, and superior tissue classification performance was observed *in vivo* (20).

This suggests that *ex vivo* human tissue lifetime data are consistent with *in vivo* fluorescence lifetime signatures, and inter-patient variability in fluorescence lifetime values may be less pronounced *in vivo*. Furthermore, in clinical practice, it is envisaged that non-cancerous tissue (in a separate lobe) would be evaluated initially, as a reference measure, and the fluorescence lifetime threshold would be adjusted during the procedure with respect to the individual, which has the potential to further optimise diagnostic accuracy.

In conclusion, our novel fibre-based FLIM system, enabling label-free high-resolution imaging and quantitative fluorescence lifetime analysis, distinguishes lung cancer, from healthy adjacent tissue *ex vivo* with good performance characteristics. Therefore, this minimally invasive technique, which permits access to distally-located lesions via existing endoscopic platforms, has potential as a real-time biopsy guidance tool, with the capability to optimise diagnostic accuracy and avoid repeated procedures in patients with early-stage lung cancer.

Footnote

Reporting Checklist: The authors have completed the STARD reporting checklist. Available at https://tlcr.amegroups.com/article/view/10.21037/tlcr-23-638/rc

Peer Review File: Available at https://tlcr.amegroups.com/article/view/10.21037/tlcr-23-638/prf

Conflicts of Interest: All authors have completed the ICMJE uniform disclosure form (available at https://tlcr.amegroups.com/article/view/10.21037/tlcr-23-638/coif). S.F. reports grant from MRC. E.W. and G.O.S.W. have patent pending relating to the imaging platform. A.R.A. received Clinician Scientist Fellowship from Cancer Research UK. K.D. reports grants from MRC, EPSRC, CARB-X and Wellcome Trust. H.S., A.R.A., J.S., K.D. and G.O.S.W. declare interests in Prothea Technologies with shares and/or employment. The other authors have no conflicts of interest to declare.

Ethical Statement: The authors are accountable for all aspects of the work in ensuring that questions related to the accuracy or integrity of any part of the work are appropriately investigated and resolved. The study was conducted in accordance with the Declaration of Helsinki (as revised in 2013). The study was approved by NHS Lothian Bioresource Research Ethics Committee (NHS Lothian, reference 15/ES/0094) and informed consent was taken from all individual participants.

References

1. Sung H, Ferlay J, Siegel RL, et al. Global Cancer Statistics 2020: GLOBOCAN Estimates of Incidence and Mortality Worldwide for 36 Cancers in 185 Countries. CA Cancer J Clin 2021;71:209-49.
2. National Lung Screening Trial Research Team, Aberle DR, Adams AM, et al. Reduced lung-cancer mortality with low-dose computed tomographic screening. N Engl J Med 2011;365:395-409.
3. Field JK, Vulkan D, Davies MPA, et al. Lung cancer mortality reduction by LDCT screening: UKLS randomised trial results and international meta-analysis. Lancet Reg Health Eur 2021;10:100179.
4. Lim E, Baldwin D, Beckles M, et al. Guidelines on the radical management of patients with lung cancer. Thorax 2010;65 Suppl 3:iii1-27.
5. Zhang W, Chen S, Dong X, et al. Meta-analysis of the diagnostic yield and safety of electromagnetic navigation bronchoscopy for lung nodules. J Thorac Dis 2015;7:799-809.
6. Chen AC, Pastis NJ, Machuzak MS, et al. Accuracy of a Robotic Endoscopic System in Cadaver Models with Simulated Tumor Targets: ACCESS Study. Respiration 2020;99:56-61.
7. Yarmus L, Hopkins Hospital FJ, Wahidi M, et al. The precision-1 study: a prospective single-blinded randomized comparative study of three guided bronchoscopic approaches for investigating pulmonary nodules. Chest 2019;156:A2256.
8. Ishida T, Asano F, Yamazaki K, et al. Virtual bronchoscopic navigation combined with endobronchial ultrasound to diagnose small peripheral pulmonary lesions: a randomised trial. Thorax 2011;66:1072-7.
9. Eberhardt R, Anantham D, Ernst A, et al. Multimodality bronchoscopic diagnosis of peripheral lung lesions: a randomized controlled trial. Am J Respir Crit Care Med 2007;176:36-41.
10. Roldán-Varona P, Ross CA, Rodríguez-Cobo L, et al. Selective plane illumination optical endomicroscopy with polymer imaging fibers. APL Photonics 2023;8:016103.
11. Wijmans L, Yared J, de Bruin DM, et al. Needle-based confocal laser endomicroscopy for real-time diagnosing and staging of lung cancer. Eur Respir J 2019;53:1801520.
12. Wijmans L, Baas P, Sieburgh TE, et al. Confocal Laser Endomicroscopy as a Guidance Tool for Pleural Biopsies in Malignant Pleural Mesothelioma. Chest 2019;156:754-63.
13. Tian S, Huang H, Zhang Y, et al. The role of confocal laser endomicroscopy in pulmonary medicine. Eur Respir Rev 2023;32:220185.
14. Mercer RR, Crapo JD. Spatial distribution of collagen and elastin fibers in the lungs. J Appl Physiol (1985) 1990;69:756-65.
15. Seth S, Akram AR, McCool P, et al. Assessing the utility of autofluorescence-based pulmonary optical endomicroscopy to predict the malignant potential of solitary pulmonary

nodules in humans. Sci Rep 2016;6:31372.

16. Marcu L. Fluorescence lifetime techniques in medical applications. Ann Biomed Eng 2012;40:304-31.

17. Mahmoud A, El-Sharkawy YH. Delineation and detection of breast cancer using novel label-free fluorescence. BMC Med Imaging 2023;23:132.

18. Kufcsák A, Erdogan A, Walker R, et al. Time-resolved spectroscopy at 19,000 lines per second using a CMOS SPAD line array enables advanced biophotonics applications. Opt Express 2017;25:11103-23.

19. Henderson R, Johnston N, Mattioli della Rocca F, et al. A 192×128 Time Correlated SPAD Image Sensor in 40-nm CMOS Technology. IEEE Journal of Solid-State Circuits 2019;54:1907-16.

20. Marsden M, Weyers B, Bec J, et al. Intraoperative Margin Assessment in Oral and Oropharyngeal Cancer Using Label-Free Fluorescence Lifetime Imaging and Machine Learning. IEEE Trans Biomed Eng 2021;68:857-68.

21. Hassan MA, Weyers B, Bec J, et al. FLIm-Based in Vivo Classification of Residual Cancer in the Surgical Cavity During Transoral Robotic Surgery. Springer, Cham; MICCAI 2023;14228.

22. Gorpas D, Phipps J, Bec J, et al. Autofluorescence lifetime augmented reality as a means for real-time robotic surgery guidance in human patients. Sci Rep 2019;9:1187.

23. Marsden M, Fukazawa T, Deng YC, et al. FLImBrush: dynamic visualization of intraoperative free-hand fiber-based fluorescence lifetime imaging. Biomed Opt Express 2020;11:5166-80.

24. Alfonso-Garcia A, Haudenschild AK, Marcu L. Label-free assessment of carotid artery biochemical composition using fiber-based fluorescence lifetime imaging. Biomed Opt Express 2018;9:4064-76.

25. Berge E, Favreau P, Heaster T, et al. Fluorescence lifetime imaging of unstained, fixed FaDu tumor slides. Proceedings Volume Label-free Biomedical Imaging and Sensing (LBIS) 2019;108901D.

26. Moore C, Chan SP, Demas JN, et al. Comparison of methods for rapid evaluation of lifetimes of exponential decays. Appl Spectrosc 2004;58:603-7.

27. Erdogan A, Walker R, Finlayson N, et al. A CMOS SPAD line sensor with per-pixel histogramming TDC for time-resolved multispectral imaging. IEEE J Solid-State Circuits 2019;54:1705-19.

28. Williams GOS, Williams E, Finlayson N, et al. Full spectrum fluorescence lifetime imaging with 0.5 nm spectral and 50 ps temporal resolution. Nat Commun 2021;12:6616.

29. Stone JM, Wood HA, Harrington K, et al. Low index contrast imaging fibers. Opt Lett 2017;42:1484-7.

30. Abbaci M, Casiraghi O, Vergez S, et al. Diagnostic accuracy of in vivo early tumor imaging from probe-based confocal laser endomicroscopy versus histologic examination in head and neck squamous cell carcinoma. Clin Oral Investig 2022;26:1823-33.

31. Ha SO, Kim DY, Sohn CH, et al. Anaphylaxis caused by intravenous fluorescein: clinical characteristics and review of literature. Intern Emerg Med 2014;9:325-30.